

Published in final edited form as:

Sci Transl Med. 2014 April 16; 6(232): 232ra52. doi:10.1126/scitranslmed.3008517.

Orally Available Small-Molecule Polymerase Inhibitor Cures a Lethal Morbillivirus Infection

Stefanie A Krumm^{1,†}, Dan Yan^{1,†}, Elise S Hovingh², Taylor J Evers³, Theresa Enkirch^{2,4}, G. Prabhakar Reddy³, Aiming Sun³, Manohar T Saindane³, Richard F Arrendale³, George Painter^{3,5}, Dennis C Liotta⁶, Michael G Natchus³, Veronika von Messling^{2,4}, and Richard K Plemper^{1,7,*}

¹Institute for Biomedical Sciences, Georgia State University, Atlanta, GA 30303

²Veterinary Medicine Division, Paul-Ehrlich-Institut, Federal Institute for Vaccines and Biomedicines, 63225 Langen, Germany

³Emory Institute for Drug Development, Emory University, Atlanta, GA 30322

⁴Emerging Infectious Disease Program, Duke-NUS Graduate Medical School, 169857 Singapore

⁵Drug Innovation Ventures at Emory, Atlanta, GA 30309

⁶Department of Chemistry, Emory University, Atlanta, GA 30322

⁷Department of Pediatrics, Emory University, Atlanta, GA 30322

Abstract

Measles virus (MeV) is a highly infectious morbillivirus responsible for major human morbidity and mortality in the non-vaccinated. The related, zoonotic canine distemper virus (CDV) induces

*To whom correspondence should be addressed: Richard K Plemper, rplemper@gsu.edu.

†These authors contributed equally to this work

List of Supplementary Materials

Materials and methods for chemical synthesis

Fig. S1. Synthesis scheme of gram-scale production of ERDRP-0519

Fig. S2. Shelf-stability assessment of ERDRP-0519

Fig. S3. Adaptation profiles of CDV strains 5804PeH and Snyder Hill

Fig. S4. ERDRP-0519 resistance sites in CDV L

Fig. S5. Comparison of different vehicle dosing regimens in control animals

Fig. S6. Clinical symptoms of treated and control animals infected with CDV-5804PeH

Fig. S7. Fever and body weight loss curves of infected animals

Fig. S8. *In vitro* resistance assessment of CDV re-isolates from four different prophylactically dosed animals.

Fig. S9. Pathogenicity comparison of CDV-5804P-mKate and CDV-5804PeH

Fig. S10. Contact transmission after single infection of source animals

Table S1. Cytotoxicity of ERDRP-0519 in immortalized cell lines and primary human PBMCs

Table S2. Oral PK profile of ERDRP-0519 in the ferret host

Author contributions: S.A.K., D.Y., E.H. and T.E. performed the experiments. A.S. and M.T.S. performed chemical synthesis. T.J.E., G.P.R. and R.F.A. performed mass-spectrometry and pharmacokinetic analyses. G.P., D.C.L., M.G.N., V.v.M. and R.K.P. provided study design. V.v.M. and R.K.P. supervised the experiments and analyzed data. R.K.P. coordinated the project and wrote the manuscript.

Competing interests: A.S. and R.K.P. are inventors on patent application PCT/US2012/030866, which includes the structure and method of use of ERDRP-0519.

Data and materials availability: Distribution of compound ERDRP-0519 for research purposes is regulated through an MTA from Emory University.

morbillivirus disease in ferrets with 100% lethality. We report an orally available, shelf-stable pan-morbillivirus inhibitor that targets the viral polymerase. Prophylactic oral treatment of ferrets infected intranasally with a lethal CDV dose reduced viremia and prolonged survival. Equally infected ferrets receiving post-infection treatment at the onset of viremia showed low-grade viral loads, remained asymptomatic and recovered from infection, while control animals succumbed to the disease. Recovered animals also mounted a robust immune response and were protected against re-challenge with a lethal CDV dose. Drug-resistant viral recombinants were generated and found attenuated and transmission impaired compared to the genetic parent. These findings pioneer a path towards an effective morbillivirus therapy that aids measles eradication by synergizing vaccine and therapeutics to close herd immunity gaps due to vaccine refusal.

Introduction

Among respiratory viruses of the *Paramyxoviridae* family, members of the morbillivirus genus such as measles virus (MeV) and canine distemper virus (CDV) are recognized for their exceptionally high attack rates, initial host invasion through lymphatic cells and organs, obligatory development of cell-associated viremia, and an extended period of immunosuppression following the primary infection (1–4). Inherently lymphotropic, morbilliviruses spread rapidly from lymphatic organs to epithelial cells and can cause neurologic complications (5, 6). Despite their overlapping disease profile, the severity and outcome of infection differ widely between individual members of the genus; for instance, the case fatality rate of MeV is approximately 1:1,000 in developed countries (5), whereas CDV is lethal in up to 50% of cases in dogs and 100% in ferrets (7), positioning the CDV/ferret system among the most lethal acute viral infections known.

Due to very efficient viral spread, a herd immunity of approximately 95% is required to prevent sporadic MeV outbreaks (8) and measles typically reemerges first when vaccination coverage in a population drops (9). Globally, major progress towards measles control was made in the 2000-2007 period, resulting in a 71%-reduction in measles mortality. However, estimated annual deaths have since plateaued at around 150,000 (10, 11). Compared to 2009, the European region reported an approximately four-fold increase to over 30,000 measles cases in 2011 (12), and high 2013 viral activity in Germany, for instance, suggests that comparably low case numbers in 2012 may not stand for a general trend reversal for that region (13). Causative are public reservations surrounding the MMR vaccine (14), which were aggravated by a fraudulent link to autism (15) and persist despite major educational efforts (16). Paradoxically, measles control suffers from its own success, since disease awareness increasingly fades from public memory as prevalence declines (17, 18). As a consequence, public risk perception changes, which leads to increasing vaccine refusal and creates a major challenge to viral eradication (19). This eroding public acceptance of continued vaccination may also trigger a future decline in immunity in regions with currently high coverage such as North America (20). While global eradication through vaccination alone is considered feasible (8, 21), a drawn-out endgame for MeV elimination will test public resolve, challenge regional control targets, and could jeopardize the ultimate success of the program (19).

Synergizing an effective therapeutic with vaccination may cut through this endgame conundrum by overcoming vaccine refusal and shortening the timeline to complete viral control. Since the disease is mostly immune-mediated (1, 9), drug intervention should reasonably concentrate on the extended latent/prodromal and early symptomatic stages of infection through post-exposure prophylaxis. Immunologically-naïve contacts of confirmed index cases are identifiable in the developed world, but post-exposure vaccination is largely ineffective (22). Predominantly prophylactic application dictates the desired drug profile: the article must be orally efficacious, ideally shelf-stable at ambient temperature, amenable to cost-effective production, and possess outstanding safety and resistance profiles. Small-molecule therapeutics are best suited to fulfill these requirements (23).

We have identified and characterized an allosteric small-molecule inhibitor class of the MeV RNA-dependent RNA-polymerase (RdRp) complex (24, 25). Hit-to-lead chemistry has produced analogs with nanomolar potency against a panel of MeV targets and compelling safety profile (26). These analogs meet key features of the desired drug product, but the identification of a clinical candidate has been hampered by the lack of a small-animal model that accurately reproduces symptoms of human MeV infection, since only primates develop a measles-like disease (27).

Pioneering the therapeutic intervention of morbillivirus infection, we implemented in this study the CDV/ferret system (28) as a surrogate assay to monitor treatment of morbillivirus infection in a natural host. Having examined ferret pharmacokinetics of a selected lead compound and its mechanism of activity against pathogenic CDV, we determined oral efficacy in ferrets intranasally infected with a lethal dose of CDV. Viral adaptation and transfer of escape mutations into a recombinant pathogenic CDV strain revealed the consequences of resistance for viral fitness and pathogenesis *in vitro* and *in vivo*.

Results

Building on a series of MeV inhibitors (25), synthetic scaffold development in preparation for this study was predominantly directed at improving oral absorption of the article to meet the desired drug properties, primarily by increasing aqueous solubility. The resulting lead ERDRP-0519 (fig. 1A) showed an excellent 39% oral availability in the rat model, high bidirectional membrane permeability (26), and was suitable for synthesis scale-up (fig. S1).

Identification of an orally available pan-morbillivirus inhibitor

Activity testing of ERDRP-0519 against a panel of MeV isolates representing clades currently endemic worldwide demonstrated continued nanomolar antiviral potency of the compound after optimization (fig. 1B and C). This favorable efficacy profile coincided with low cytotoxicity in established human and animal cell lines and primary human PBMCs (table S1), resulting in selectivity indices (SI) >200 against all MeV targets analyzed. The indication spectrum of the compound extended to pathogenic CDV strains, recombinant CDV-5804PeH (4, 29) and the neuroadapted Snyder Hill isolate (30), albeit with potency reduced approximately 2-fold (fig. 1C). To explore suitability of the ferret host for efficacy testing, we determined PK parameters after single-dose oral administration (fig. 1D and table S2). Peak plasma concentrations exceeded 1,500 ng/ml (corresponding to

approximately 3.5 μM) and reached thus about 5-times the *in vitro* EC_{50} concentration of CDV-5804PeH. Serum protein binding of ERDRP-0519 was <95%, and shelf-stability at ambient temperature exceeded one year without loss of activity (fig. S2), making ERDRP-0519 a promising candidate for morbillivirus therapy.

ERDRP-0519 targets the morbillivirus polymerase complex

Compounds of the ERDRP-0519 class block activity of the MeV RdRp complex (24). To determine whether this mechanism of activity extends to CDV polymerase, we compared the compound in subinfection replicon reporter assays established for MeV (31), CDV, and a distant member of the paramyxovirus family, respiratory syncytial virus (RSV) (32). Both morbillivirus-derived polymerase complexes were potently inhibited by ERDRP-0519, while the RSV replicon was not blocked, confirming morbillivirus-specific, dose-dependent inhibition of RdRp activity (fig. 2A).

Adaptation of MeV to growth in the presence of this compound class has identified several hot-spots of resistance in the viral L protein, the catalytically active subunit of the polymerase complex. Most prominently, we found that several escape mutants framed a GDNQ motif in L that is considered the active center for phosphodiester bond formation (33). To address whether inhibition of MeV and CDV RdRp complexes by ERDRP-0519 is based on comparable docking poses, we generated escape variants of CDV strains Snyder Hill and 5804P (fig. S3). Candidate mutations identified in nine discrete adaptation campaigns were rebuilt individually in the CDV replicon system, followed by inhibition testing (fig. S4). This procedure highlighted eight substitutions affecting six discrete positions in CDV L that improved bioactivity in the presence of the inhibitor compared to unmodified CDV L (fig. 2B).

For each resistance site identified, we transferred one substitution into a cDNA copy of the CDV-5804P genome (4, 29) and recovered the corresponding CDVs. All recombinants contained an additional eGFP open reading frame, which does not impair pathogenicity of the virus in ferrets (4). Dose-response curves (fig. 2C) revealed robust resistance of CDV-5804PeH-L_{T751I} and L_{T776A} (EC_{90} concentrations increased >20-fold), intermediate resistance of CDV-5804PeH-L_{H589Y}, L_{H816L}, and L_{G835R} (EC_{90} concentrations increased approximately 8-fold), and moderate resistance of CDV-5804PeH-L_{N398D} (approximately 2-fold increase in EC_{90} concentration). We noted high consistency in the location of escape sites between CDV and MeV. Escape mutations mapped to the amino-terminal half of the L protein and resistance sites 589 and 776, the latter bordering the GDNQ motif, were identical in both pathogens (fig. 2B).

Oral efficacy against a lethal morbillivirus infection

Having established mechanistic reproducibility between different morbillivirus targets, we employed the CDV/ferret system to assess efficacy of anti-morbillivirus therapy in a natural host. We administered ERDRP-0519 orally at 50 mg/kg body mass b.i.d., following either a prophylactic or post-exposure therapeutic (PET) study protocol. For the former, dosing was initiated 24 hours pre-infection, while the latter commenced at the onset of viremia, three days post-infection, and was continued for 14 days (fig. 3A). Control group received vehicle

only, following the prophylactic protocol, since comparison tests confirmed that the vehicle dosing regimen has no effect on disease progression and viremia titers (fig. S5).

All animals were infected intranasally with 1×10^5 TCID₅₀ units of CDV-5804PeH, which corresponds to approximately 10 LD₅₀ (29). Vehicle-treated ferrets developed viremia three days post-infection, showed first clinical signs of morbillivirus disease such as rash and fever at day seven, and succumbed to the disease after approximately 12-15 days (4, 29). Prophylactic treatment significantly prolonged animal survival, reduced viral load and delayed lymphopenia (fig. 3B-D).

Remarkably, PET dosing resulted in complete survival of infected animals (fig. 3B). All ferrets showed an approximately 99% reduction in virus load and experienced only mild, transient lymphocyte depletion (fig. 3C and D). Consistent with the results of our single-dose PK studies in rats and ferrets, plasma analysis revealed robust, micromolar steady-state levels of the drug (fig. 3E). PBMC responsiveness was only transiently impaired in the PET group, intermediately reduced in the prophylactically treated animals, but essentially abrogated in the vehicle-treated controls (fig. 3F).

Quantification of type I interferon and Mx1 (ISG representative) induction levels in PBMCs isolated from animals of each treatment group revealed robust stimulation of the host interferon response in the PET dosing group at day 7 post-infection, when virus replication was impaired by the compound (figure 3G). By contrast, animals of the vehicle control group lacked a comparable innate response, consistent with host immune suppression by the viral V protein (34). Efficient suppression of virus replication at all times in prophylactically treated animals was reflected by low interferon induction levels.

Lasting immunoprotection against morbillivirus infection is antibody-mediated (9). Importantly, ferrets in the PET group remained subclinical (fig. S6 and S7) and mounted a strong humoral response with neutralizing antibodies first detectable seven days post-infection, followed by a rapid increase in neutralizing titer (fig. 3H). All animals of this group were fully protected against a lethal CDV challenge with 10 LD₅₀, administered 35 days after the original infection and 18 days after completion of treatment.

Effect of viral resistance to ERDRP-0519 on pathogenicity

Allosteric polymerase inhibitors are compromised for antiretroviral therapy by the rapid development of resistance in chronic infections (35). However, morbilliviruses predominantly cause acute disease and all therapeutically dosed animals completely cleared the infection by day 28 pI, ruling out viral escape. Likewise, none of four re-isolates from the prophylactic group showed robust resistance (fig. S8). We therefore employed the resistant recombinants generated *in vitro* to assess the effect of escape from ERDP-0519 on relative viral fitness. To establish an *in vitro* competition assay (fig. 4A), we exchanged the eGFP open reading frame in CDV-5804PeH for that of far-red fluorescent mKate2 and recovered the corresponding CDV-5804P-mKate. Infection of ferrets confirmed indistinguishable pathogenicity of this recombinant and CDV-5804PeH (fig. S9). In three independent replicates each, cells were then co-infected with equal amounts of compound-sensitive CDV-5804P-mKate and one of the six confirmed resistant mutants in the

CDV-5804PeH background. Viruses were passaged eight times, and the relative prevalence of standard and resistant virus quantified by fluorescence pattern.

Of the six resistance sites identified, three recombinants (751, 816, and 835) were outgrown by the parental virus, and a fourth site (398) also showed no significant improvement of relative viral fitness (fig. 4B). Two resistant variants (589 and 776), however, reproducibly outgrew the unmodified virus, evidenced by a significant overrepresentation of green fluorescence after eight passages. Sequence analysis confirmed that the presence of viral genomes encoding mutant L proteins at conclusion of the experiment. Substitutions at L positions 589 and 776 likewise mediated escape of MeV L from this compound class (24), identifying them as conserved hot-spots of morbillivirus resistance to the inhibitor with potential to also emerge in the human host.

To address whether the resistance mutations affect virulence, we infected ferrets with these two recombinants, either singly or together with an equal amount of standard CDV-5804P-mKate particles. For comparison, we included CDV-5804PeH-L_{T751I}, since this substitution resulted in attenuation *in vitro* but likewise was in close proximity to the previously identified escape sites in MeV L.

All animals infected with the parental virus experienced typical disease progression characterized by potent viremia with peak viral loads ten days post-infection and death of all infected animals within a 14-day period (fig. 4C and D). Of the escape mutants, only CDV-5804PeH-L_{T776A} induced lethal disease and viremia resembling that of the standard virus. However, median survival of CDV-5804PeH-L_{T776A}-infected animals survived for up to 21 days, indicating mild attenuation. By contrast, resistant CDV-5804PeH-L_{H589Y} and CDV-5804PeH-L_{T751I} were both attenuated, manifested by lower grade viremia and recovery of most/all animals of both groups from infection (fig. 4 C and D). Coinfection of animals with equal amounts of parental and either of the different resistant viruses did not enhance disease (fig. 4E).

To assess possible spread of viral resistance, we performed contact transmission studies with CDV-5804PeH-L_{T776A}, which was the least attenuated of all resistant viruses tested *in vivo*. Source animals were infected either singly or co-infected with equal doses of standard and resistant virus, followed by co-habitation with uninfected contact animals. Ferrets infected with CDV-5804PeH-L_{T776A} alone transmitted the virus to cage contacts, but disease progression in the contact animals was delayed compared to that after transmission of the parent virus (fig. 4F and fig. S10). After co-infection of the source animals with resistant and sensitive viruses, viremia titers of resistant CDV-5804PeH-L_{T776A} were reduced in the contact animals compared to those of the sensitive reference virus (Fig 4G). These observations indicate a lower transmission success rate of the resistant CDV-5804PeH-L_{T776A} than the standard virus, and alleviate concerns that viral escape from inhibition may increase disease severity or induce genetic drift in endemic virus populations.

Discussion

We have pioneered the development of an orally available small-molecule morbillivirus polymerase inhibitor that is capable of curing a lethal morbillivirus infection when administered at the first onset of viremia. Low cytotoxicity in cultured and primary human cells and promising PK parameters recommend this compound for further development in preparation of clinical testing for human or veterinary therapy.

The level of viremia reduction (~99%) observed after prophylactic or therapeutic dosing with the clinical candidate is groundbreaking in the CDV/ferret system. This can be attributed to the favorable pharmacological properties of the compound after repeated oral dosing. Closely overlapping ferret, rat, and human cell-based metabolic profiles of the scaffold (26) suggest that these favorable characteristics may equally extend to human therapy.

Several lines of evidence support a conserved inhibitory mechanism and docking pose with the viral polymerase between the MeV and CDV targets. First, the compound class specifically blocks RdRp activity of both CDV and MeV; second, the molecular basis for resistance to this class was traced to the L subunit of the CDV and MeV (24) polymerase complex; and, third, two hot-spots of resistance were fully conserved between the different scaffold analogs and morbillivirus targets (24). These findings validate the CDV/ferret system as a relevant model for efficacy assessment.

Our study indicates that post-exposure treatment commencing at the onset of viremia primes a robust immune response through initially unimpaired replication of a non-attenuated pathogenic virus. Uncontrolled, morbillivirus replication induces lymphopenia in experimental (2, 4) and clinical (1, 3) settings; in the CDV/ferret system, adaptive immunity collapses and the host succumbs to the disease before immune control can be established. We hypothesize that under post-exposure therapy, inhibition of virus replication at the onset of viremia takes full advantage of initial immune priming. The subsequent pharmacological attenuation of the virus, however, prevents immune collapse and allows a robust induction of the innate host antiviral response. Suppressed lymphopenia and lymphocyte unresponsiveness opens a window for the generation of a robust host antiviral response, leading to viral clearance and high neutralizing antibody titers. Consistent with this reaction, all PET dosed animals were after recovery fully protected against re-challenge with a lethal CDV dose. In the absence of strong initial immune stimulation through freely replicating pathogenic virus, the drug is efficacious but insufficient to prevent host immune-collapse in a disease situation as extreme as the CDV/ferret system, despite a reduction in viremia, delayed lymphopenia, and alleviated lymphocyte unresponsiveness. This differential response to prophylactic versus PET dosing showcases a critical role of the very early phase of morbillivirus infection in immune dynamics and disease outcome, which is discussed for a variety of acute respiratory virus infections (36). Our results underscore that clinical benefit of therapeutic intervention will best be achieved in conjunction with a competent innate host immune response.

The CDV/ferret-based findings allow five major extrapolations to the MeV/human disease problem, given the conservation of key infection features among morbilliviruses (4, 37):

i) Efficacy; post-exposure treatment commencing during the prodromal phase of MeV infection has high potential for clinical success, characterized by an asymptomatic course of infection and the induction of robust, protective immunity. We have not yet monitored surviving ferrets over extended time periods, but consider it likely that the extensive immunosuppression phase following morbillivirus infection (3, 28) may also be alleviated or eliminated. Based on a 10 to 14-day latent and prodromal phase of MeV in humans, we anticipate that a 14-day oral treatment cycle of immunologically-naïve contacts of a confirmed index case will recapitulate the efficacy seen in the CDV/ferret surrogate. We have not observed signs of compound-induced toxicity in the PET group, and are confident that higher *in vitro* sensitivity of MeV than CDV to ERDRP-0519 will allow even lower dosing for human therapy.

ii) Immune response; it is well documented that vaccine-induced protection against MeV infection is less robust than naturally acquired immunity (38). All therapeutically treated ferrets were fully protected against a lethal CDV challenge dose, indicating that infection with non-attenuated MeV followed by pharmaceutical virus attenuation through ERDRP-0519 induces robust immunity. This observation outlines the potential impact of treatment on MeV eradication efforts; preventing symptomatic disease in the unvaccinated, blocking viral spread in local outbreak areas, and contributing to closing herd immunity gaps due to vaccine refusal as currently experienced in Europe.

iii) Disease management; measles is largely an immunologic disease and viral titers in infected individuals decline rapidly after the onset of symptoms (8). Due to faster onset of CDV disease in ferrets than measles in humans, we expect efficacy tests exploring initiation of treatment during the prodromal phase to be problematic to interpret in the CDV/ferret system. While the full efficacy time window for therapeutic intervention should therefore be evaluated in the MeV/primate model, we would expect little impact when treatment is initiated subsequent to rash. Consequently, therapeutic effort is best directed at contacts of an index case, who are still in the prodromal or very early symptomatic phase. However, we anticipate therapy to improve management of complications involving persistent infection, such as measles inclusion body encephalitis in the immunocompromised (39).

iv) Prophylaxis; pre-exposure prophylaxis of ferrets must be evaluated in the context of an exceptionally severe disease phenotype. We consider it likely that proven drug efficacy in the form of substantially prolonged (up to 2-fold) survival of treated ferrets observed in our study will translate into mild, or entirely asymptomatic, presentation of the more moderate MeV disease experienced in humans. Moreover, prophylactically treated ferrets eventually initiated a neutralizing antibody response and showed a milder lymphocyte proliferation arrest. These results alleviate concerns that prophylactic treatment may predispose for severe disease as experienced with a formalin-inactivated MeV vaccine in the 1960s (40), since this “atypical measles” syndrome was due to failed affinity maturation, resulting in nonprotective antibodies and immune complex deposition (41).

v) Resistance; viral adaptation revealed that escape from ERDRP-0519 inhibition coincides with attenuation. We furthermore found no evidence for enhanced disease in the presence of wild type and resistant virus, or superior transmission rates of resistant virus. Since hot-spots of resistance are conserved between CDV and MeV, similar molecular escape profiles can be anticipated clinically. Morbilliviruses predominantly cause acute disease, followed by rapid immune-mediated viral clearance, mandating high-frequency transmission to sustain the infection in a population (42). Based on the absence of secondary transmission of the attenuated measles vaccine (8) and preferential transmission of standard virus from co-infected animals, we propose that in the context of acute morbillivirus disease, attenuated resistant virions will likely remain clinically insignificant.

Beyond the morbillivirus system, our data provide proof-of-concept for the currently unexplored clinical potential of allosteric polymerase inhibitors for the treatment of acute viral infections. The clinical candidate is in principle suitable for veterinary and human use. However, effective suppression of symptomatic disease and the development of robust antiviral immunity after post-exposure treatment predestine the compound as a second weapon in our struggle for the endgame of global MeV eradication.

Materials and Methods

Study design

This study established the CDV/ferret model as a surrogate system to assess the efficacy and resistance package of an anti-measles virus therapeutic candidate. After mechanistic characterization of the compound against the CDV target *in vitro* and the development of an oral PK profile for the ferret host, the effect of different dosing regimens on animal survival, viremia titers, induction of innate host immune responses and immune suppression, and the development of protective immunity was determined. Resistance was induced through viral adaptation, genetically controlled resistant CDV recombinants were generated and their relative fitness, pathogenicity, and potential for transmission assessed *in vitro* and *in vivo*. Animals were assigned randomly to the different treatment groups. Specific information regarding sampling and replication of individual assays is provided in the figure legends.

Cell culture and viruses

All cell lines were maintained at 37°C and 5% CO₂ in Dulbecco's modified Eagle's medium supplemented with 7.5% fetal bovine serum. Vero (African green monkey kidney epithelial) cells (ATCC CCL-81) stably expressing human or canine signaling lymphocytic activation molecule (Vero-hSLAM cells and Vero-cSLAM cells (43), respectively) and baby hamster kidney (BHK-21) cells stably expressing T7 polymerase (BSR-T7/5 (BHK-T7) cells) received 500 µg/ml G-418 (Geneticin) for selection. Human peripheral blood mononuclear cells (PBMCs) were prepared and stimulated as previously described (31). Lipofectamine 2000 (Invitrogen) was used for transfections. Virus strains used in this study were recombinant MeV-Edmonston (recMeV) and endemic typing strains MV_i/Ibadan.NIE/97/1 [B3-2], MV_i/Maryland.USA/77 [C2-1], MV_i/Illinois.USA/46.02 [D3], MV_i/New Jersey.USA/94/1 [D6], MV_i/Illinois.USA/50.99 [D7-2], and MV_i/Alaska.USA/16.00 [H] (genotypes in parentheses), and neuroadapted CDV isolate Snyder Hill (30) and

CDV-5804PeH, which is based on the CDV-5804Han89 isolate (29). MeV and CDV stocks were grown and titrated through TCID₅₀ titration on Vero-hSLAM and Vero-cSLAM cells, respectively.

Compound synthesis and formulation

Compound synthesis was carried out as described (26) with the modifications specified in supplements. Compound was dissolved in DMSO for cell culture studies, and formulated in PEG200/0.5% methylcellulose (10/90) for *in vivo* dosing.

In vitro efficacy testing

Cells were infected with MeV or CDV strains (MOI 0.1 TCID₅₀/cell) in the presence of three-fold serial compound dilutions (30 µM highest) or vehicle, and incubated with compound until vehicle controls showed 90% CPE. Cell-associated progeny particles were titered and inhibitory concentrations calculated through four-parameter variable slope non-linear regression fitting.

Assessment of compound cytotoxicity

A CytoTox96 non-radioactive cytotoxicity assay (Promega) was used to quantify toxicity (highest concentration assessed 75 µM). Values were normalized for vehicle controls according to %-toxicity = $100 - ((\text{specific}_{490\text{nm}}) / (\text{vehicle}_{650\text{nm}}) * 100)$. To calculate CC₅₀ concentrations, mean values of four replicates were analyzed.

Pharmacokinetics profiling

Ferrets were dosed p.o. with ERDRP-0519, followed by blood sampling. Plasma was purified from heparinized blood and drug concentrations determined using internal standard, reversed phase isocratic HPLC method with positive ion electrospray ionization (ESI) mass spectrometry detection (LC/MS/MS) on an AB-SCIEX API 4000 MS/MS instrument (5 µl injection volume). Pharmacokinetic parameters were estimated using WinNonlin 5.3 (Pharsight).

Replicon reporter assays

Luciferase replicon reporter systems for MeV, CDV and respiratory syncytial virus (RSV) were described previously (29, 31, 32). Reporter activities were determined in the presence of three-fold serial dilutions of ERDRP-0519 (10 µM highest). Luciferase activities in cell lysates were measured in a Synergy H1 microplate reader (BioTek) in top-count mode. Inhibitory concentrations were calculated through four-parameter variable slope regression modeling.

In vitro virus adaptation

Vero-cSLAM cells were infected with CDV strains Snyder Hill or 5804PeH at an MOI of 0.1 TCID₅₀/cell and incubated in the presence of ERDRP-0519 starting at 0.5 µM. When extensive viral CPE was detected, cell-associated viral particles were released, diluted 20-fold and used for re-infection in the presence of increased compound concentrations.

RT-PCR and sequencing of viral cDNAs

RNA was extracted using the RNeasy mini kit (Qiagen) and cDNAs created using random hexamer primers and Superscript III reverse transcriptase (Invitrogen). Modified genome regions were amplified using appropriate primers and subjected to cDNA sequencing.

Molecular biology and recovery of recombinant CDV

Candidate resistance mutations were rebuilt in a pTM1-CDV-L expression plasmid (29) and subjected to replicon reporter assays for confirmation. The QuikChange protocol (Stratagene) was applied for all site-directed mutagenesis reactions. Confirmed escape mutations were transferred into a full-length cDNA clone of the CDV-5804PeH genome (4). To generate CDV-5804P-mKate, the eGFP open reading frame in p(+)-CDV-5804PeH was replaced with an equivalent fragment containing mKate2 and the resulting genomic p(+)-CDV-5804P-mKate plasmid corrected for the paramyxovirus rule-of-six. All recombinant CDV virions were recovered following a general strategy optimized for MeV (24). The presence of engineered point mutations in recovered virions was confirmed through RT-PCR and cDNA sequencing.

In vivo efficacy testing

Male and female adult European ferrets (*Mustela putorius furo*) without immunity against CDV were used in this study. All animal experiments were approved by the SingHealth IACUC Committee or were carried out in compliance with the regulations of the German animal protection law. For efficacy studies, animals were infected intranasally with 1×10^5 TCID₅₀ of CDV-5804PeH/animal and treated with ERDRP-0519 via gastric gavage at 50 mg/kg body mass as specified. Gavage tubes were flushed with 5 ml of a high caloric fluid. Blood samples were collected from the jugular vein and the animals were weighed on days 0, 3, 7, 10, 14, and weekly thereafter. All animals were observed daily for clinical signs.

For white blood cell counts, 10 μ l of heparinized blood was diluted in 990 μ l 3% acetic acid. Prior to Ficoll gradient centrifugation (GE Healthcare), plasma was collected for the quantification of drug concentrations and neutralizing antibodies. To quantify cell-associated viremia, total white blood cells were isolated and added to Vero-cSLAM cells in tenfold dilution steps. To assess proliferation activity of isolated PBMCs, cells were stimulated with 0.2 μ g phytohemagglutinin (PHA, Sigma) for 24 hours, followed by addition of 10 μ M 5-bromo-2'-deoxyuridine (BrdU, Roche). After a 24-hour incubation period, cells were fixed and BrdU incorporation quantified using a peroxidase-linked anti-BrdU antibody in a chemiluminescence assay. Signals were detected in a microplate luminescence counter (Pherastar), and the extent of proliferation expressed as the ratio of non-stimulated to stimulated cells. Neutralizing antibodies were quantified by mixing two-fold plasma dilutions starting at 1:10 with 10^2 TCID₅₀ of CDV-5804PeH for 30 min before adding Vero-cSLAM cells. Neutralizing antibody titers were expressed as reciprocal values of the last dilution without syncytia formation.

mRNA induction analysis

Relative IFN α , β , and Mx1 mRNA induction levels in PBMCs were determined by semi-quantitative real-time PCR analysis as described previously (44). RNA was isolated from PBMCs collected on days 0, 3, and 7 post-infection, and the corresponding cDNAs subjected to real-time PCR using a QuantiTect SYBR Green PCR master mix (Qiagen). GAPDH mRNA served as an internal reference, and mRNA induction levels were normalized to day 0 values. Relative change in transcription levels was calculated using the formula [fold change = $2^{-\Delta\Delta C_t}$] (45).

In vitro fitness competition assay

Vero-cSLAM cells were infected with CDV-5804P-mKate and one of the resistant mutants in the CDV-5804PeH background at an MOI of 0.01 TCID₅₀/cell each. When CPE reached >80%, cell-associated progeny virions were harvested, diluted 5,000-fold, and used for infection of fresh Vero-cSLAM cells. Of each passage, viral titers were determined. At the specified passage numbers, Vero cells were infected at an MOI of 0.1 TCID₅₀/cell through spin-inoculation (30 minutes, 1,500 rpm, 4°C). Three days post-infection, eGFP and mKate2 fluorescence of individual infectious centers determined using a Zeiss Axio Observer fluorescence microscope. For each passage and independent competition infection, at least 50 distinct infectious centers were analyzed. After eight passages, RNA was extracted from infected cells and subjected to RT-PCR and cDNA sequencing.

In vivo pathogenesis

Ferrets were infected with 2×10^5 TCID₅₀ of CDV-5804PeH or a resistant variant in the CDV-5804PeH background. Disease progression was monitored as above. For *in vivo* fitness testing, ferrets were infected intranasally with 2×10^5 TCID₅₀/animal of CDV-5804P-mKate, or co-infected with 1×10^5 TCID₅₀/animal each of CDV-5804P-mKate and a resistant variant in the CDV-5804PeH background. Disease progression was monitored as above, and viremia titers determined independently based on eGFP and mKate2 fluorescence using a Zeiss Axio Vert.A1 fluorescence microscope.

Statistical analysis

To determine active concentrations from dose-response curves, four parameter variable slope regression modeling was performed using the Prism (GraphPad) software package. Results were expressed as 50% or 90% inhibitory concentrations with 95% asymmetrical confidence intervals. To assess the statistical significance of differences between sample means, unpaired two-tailed t-tests were applied. Statistical significance of differences between treatment groups was assessed by analysis of variance (ANOVA) in combination with multiple comparison tests as specified in the figure legends. Survival curves were analyzed using a log-rank (Mantel-Cox) test. Experimental uncertainties are identified by error bars, representing standard deviation (SD) or standard error of the mean (SEM) as specified.

Supplementary Material

Refer to Web version on PubMed Central for supplementary material.

Acknowledgments

We thank P.A.Rota for providing MeV typing strains from the collection of the CDC, M.L.Moore for RSV replicon plasmids, Y.Yanagi for Vero-hSLAM and Vero-cSLAM cell lines, and M.L.Moore and A.L.Hammond for comments on the manuscript.

Funding: E.H. received an Erasmus Scholarship. This work was supported by a Duke-NUS Signature Research Program start-up grant by the Agency for Science, Technology and Research, Ministry of Health, Singapore, funding from the German Ministry of Health (to V.v.M.), and by Public Health Service grants AI071002 and AI057157 from the NIH/NIAID (to R.K.P.).

References

1. de Vries RD, Mesman AW, Geijtenbeek TB, Duprex WP, de Swart RL. The pathogenesis of measles. *Curr Opin Virol.* 2012; 2:248–255. [PubMed: 22483507]
2. de Vries RD, McQuaid S, van Amerongen G, Yuksel S, Verburgh RJ, Osterhaus AD, Duprex WP, de Swart RL. Measles immune suppression: lessons from the macaque model. *PLoS Pathog.* 2012; 8:e1002885. [PubMed: 22952446]
3. Griffin DE. Measles virus-induced suppression of immune responses. *Immunol Rev.* 2010; 236:176–189. [PubMed: 20636817]
4. von Messling V, Milosevic D, Cattaneo R. Tropism illuminated: lymphocyte-based pathways blazed by lethal morbillivirus through the host immune system. *Proc Natl Acad Sci U S A.* 2004; 101:14216–14221. [PubMed: 15377791]
5. Perry RT, Halsey NA. The clinical significance of measles: a review. *J Infect Dis.* 2004; 189(Suppl 1):S4–S16. [PubMed: 15106083]
6. Ludlow M, Nguyen DT, Silin D, Lyubomska O, de Vries RD, von Messling V, McQuaid S, De Swart RL, Duprex WP. Recombinant canine distemper virus strain Snyder Hill expressing green or red fluorescent proteins causes meningoencephalitis in the ferret. *J Virol.* 2012; 86:7508–7519. [PubMed: 22553334]
7. Davidson M. Canine distemper, virus infection in the domestic ferret. *Compend. Contin. Educ. Pract. Vet.* 1986; 8:448–453.
8. Moss WJ, Griffin DE. Global measles elimination. *Nat Rev Microbiol.* 2006; 4:900–908. [PubMed: 17088933]
9. Moss WJ, Griffin DE. Measles. *Lancet.* 2012; 379:153–164. [PubMed: 21855993]
10. WHO. Measles. 2013. <http://www.who.int/mediacentre/factsheets/fs286/en/index.html>
11. Simons E, Ferrari M, Fricks J, Wannemuehler K, Anand A, Burton A, Strebel P. Assessment of the 2010 global measles mortality reduction goal: results from a model of surveillance data. *Lancet.* 2012; 379:2173–2178. [PubMed: 22534001]
12. European Center for Disease Control and Prevention. Number of measles cases, 2011. 2011 http://ecdc.europa.eu/en/healthtopics/measles/epidemiological_data/Pages/Number-of-measles-cases-2011.aspx.
13. Santibanez S, Mankertz A. [Molecular surveillance shows progress in measles elimination process]. *Bundesgesundheitsblatt Gesundheitsforschung Gesundheitsschutz.* 2013; 56:1238–1242. [PubMed: 23990085]
14. Larson HJ, Cooper LZ, Eskola J, Katz SL, Ratzan S. Addressing the vaccine confidence gap. *Lancet.* 2011; 378:526–535. [PubMed: 21664679]
15. Murch SH, Anthony A, Casson DH, Malik M, Berelowitz M, Dhillon AP, Thomson MA, Valentine A, Davies SE, Walker-Smith JA. Retraction of an interpretation. *Lancet.* 2004; 363:750. [PubMed: 15016483]
16. Goodson JL, Chu SY, Rota PA, Moss WJ, Featherstone DA, Vijayaraghavan M, Thompson KM, Martin R, Reef S, Strebel PM. Research priorities for global measles and rubella control and eradication. *Vaccine.* 2012; 30:4709–4716. [PubMed: 22549089]
17. Brown KF, Long SJ, Ramsay M, Hudson MJ, Green J, Vincent CA, Kroll JS, Fraser G, Sevdalis N. UK parents' decision-making about measles-mumps-rubella (MMR) vaccine 10 years after the

- MMR-autism controversy: a qualitative analysis. *Vaccine*. 2012; 30:1855–1864. [PubMed: 22230590]
18. Smith PJ, Humiston SG, Marcuse EK, Zhao Z, Dorell CG, Howes C, Hibbs B. Parental delay or refusal of vaccine doses, childhood vaccination coverage at 24 months of age, and the Health Belief Model. *Public Health Rep*. 2011; 126(Suppl 2):135–146. [PubMed: 21812176]
 19. Saint-Victor DS, Omer SB. Vaccine refusal and the endgame: walking the last mile first. *Philos Trans R Soc Lond B Biol Sci*. 2013; 368:20120148. [PubMed: 23798696]
 20. Centers for Disease Control and Prevention, Measles - United States, 2011. *MMWR Morb Mortal Wkly Rep*. 2012; 61:253–257. [PubMed: 22513526]
 21. Orenstein WA, Hinman AR. Measles: the burden of preventable deaths. *Lancet*. 2012; 379:2130–2131. [PubMed: 22534000]
 22. Rice P, Young Y, Cohen B, Ramsay M. MMR immunisation after contact with measles virus. *Lancet*. 2004; 363:569–570. [PubMed: 14975626]
 23. Ganellin, CR.; Jefferis, R.; Roberts, SM., editors. Introduction to biological and small molecule drug research and development : theory and case studies. Vol. ume. Oxford: Academic Press; 2013. p. 1
 24. Yoon JJ, Krumm SA, Ndungu JM, Hoffman V, Bankamp B, Rota PA, Sun A, Snyder JP, Plemper RK. Target analysis of the experimental measles therapeutic AS-136A. *Antimicrob Agents Chemother*. 2009; 53:3860–3870. [PubMed: 19528268]
 25. White LK, Yoon JJ, Lee JK, Sun A, Du Y, Fu H, Snyder JP, Plemper RK. Nonnucleoside inhibitor of measles virus RNA-dependent RNA polymerase complex activity. *Antimicrob Agents Chemother*. 2007; 51:2293–2303. [PubMed: 17470652]
 26. Ndungu JM, Krumm SA, Yan D, Arrendale RF, Reddy GP, Evers T, Howard R, Natchus MG, Saindane MT, Liotta DC, Plemper RK, Snyder JP, Sun A. Non-nucleoside inhibitors of the measles virus RNA-dependent RNA polymerase: synthesis, structure-activity relationships, and pharmacokinetics. *J Med Chem*. 2012; 55:4220–4230. [PubMed: 22480182]
 27. Auwaerter PG, Rota PA, Elkins WR, Adams RJ, DeLozier T, Shi Y, Bellini WJ, Murphy BR, Griffin DE. Measles virus infection in rhesus macaques: altered immune responses and comparison of the virulence of six different virus strains. *J Infect Dis*. 1999; 180:950–958. [PubMed: 10479117]
 28. Pillet S, Svitek N, von Messling V. Ferrets as a model for morbillivirus pathogenesis, complications, and vaccines. *Curr Top Microbiol Immunol*. 2009; 330:73–87. [PubMed: 19203105]
 29. von Messling V, Springfield C, Devaux P, Cattaneo R. A ferret model of canine distemper virus virulence and immunosuppression. *J Virol*. 2003; 77:12579–12591. [PubMed: 14610181]
 30. Gillespie JH, Rickard CG. Encephalitis in dogs produced by distemper virus. *Am J Vet Res*. 1956; 17:103–108. [PubMed: 13283234]
 31. Krumm SA, Ndungu JM, Yoon JJ, Dochow M, Sun A, Natchus M, Snyder JP, Plemper RK. Potent host-directed small-molecule inhibitors of myxovirus RNA-dependent RNA-polymerases. *PLoS One*. 2011; 6:e20069. [PubMed: 21603574]
 32. Hotard AL, Shaikh FY, Lee S, Yan D, Teng MN, Plemper RK, Crowe JE Jr, Moore ML. A stabilized respiratory syncytial virus reverse genetics system amenable to recombination-mediated mutagenesis. *Virology*. 2012; 434:129–136. [PubMed: 23062737]
 33. Chattopadhyay A, Raha T, Shaila MS. Effect of single amino acid mutations in the conserved GDNQ motif of L protein of Rinderpest virus on RNA synthesis in vitro and in vivo. *Virus Res*. 2004; 99:139–145. [PubMed: 14749179]
 34. Svitek N, Gerhauer I, Goncalves C, Grabski E, Doring M, Kalinke U, Anderson DE, Cattaneo R, von Messling V. Morbillivirus Control of the Interferon Response: Relevance of STAT2 and mda5 but not STAT1 for Canine Distemper Virus Virulence in Ferrets. *J Virol*. 2013; 88:2941–2950. [PubMed: 24371065]
 35. De Clercq E. Non-nucleoside reverse transcriptase inhibitors (NNRTIs): past, present, and future. *Chem Biodivers*. 2004; 1:44–64. [PubMed: 17191775]

36. Tisoncik JR, Korth MJ, Simmons CP, Farrar J, Martin TR, Katze MG. Into the eye of the cytokine storm. *Microbiology and molecular biology reviews: MMBR*. 2012; 76:16–32. [PubMed: 22390970]
37. Lemon K, de Vries RD, Mesman AW, McQuaid S, van Amerongen G, Yuksel S, Ludlow M, Rennick LJ, Kuiken T, Rima BK, Geijtenbeek TB, Osterhaus AD, Duprex WP, de Swart RL. Early target cells of measles virus after aerosol infection of non-human primates. *PLoS Pathog*. 2011; 7:e1001263. [PubMed: 21304593]
38. Mossong J, O'Callaghan CJ, Ratnam S. Modelling antibody response to measles vaccine and subsequent waning of immunity in a low exposure population. *Vaccine*. 2000; 19:523–529. [PubMed: 11027817]
39. Hardie DR, Albertyn C, Heckmann JM, Smuts HE. Molecular characterisation of virus in the brains of patients with measles inclusion body encephalitis (MIBE). *Virology*. 2013; 453:283–291. [PubMed: 24025157]
40. Carter CH, Conway TJ, Cornfeld D, Iezzoni DG, Kempe CH, Moscovici C, Rauh LW, Vignec AJ, Warren J. Serologic response of children to inactivated measles vaccine. *JAMA*. 1962; 179:848–853. [PubMed: 13876943]
41. Polack FP, Hoffman SJ, Crujeiras G, Griffin DE. A role for nonprotective complement-fixing antibodies with low avidity for measles virus in atypical measles. *Nature Med*. 2003; 9:1209–1213. [PubMed: 12925847]
42. Keeling MJ, Grenfell BT. Disease extinction and community size: modeling the persistence of measles. *Science*. 1997; 275:65–67. [PubMed: 8974392]
43. Seki F, Ono N, Yamaguchi R, Yanagi Y. Efficient isolation of wild strains of canine distemper virus in Vero cells expressing canine SLAM (CD150) and their adaptability to marmoset B95a cells. *J Virol*. 2003; 77:9943–9950. [PubMed: 12941904]
44. Svitek N, von Messling V. Early cytokine mRNA expression profiles predict Morbillivirus disease outcome in ferrets. *Virology*. 2007; 362:404–410. [PubMed: 17289104]
45. Schmittgen TD, Zakrajsek BA, Mills AG, Gorn V, Singer MJ, Reed MW. Quantitative reverse transcription-polymerase chain reaction to study mRNA decay: comparison of endpoint and real-time methods. *Anal Biochem*. 2000; 285:194–204. [PubMed: 11017702]

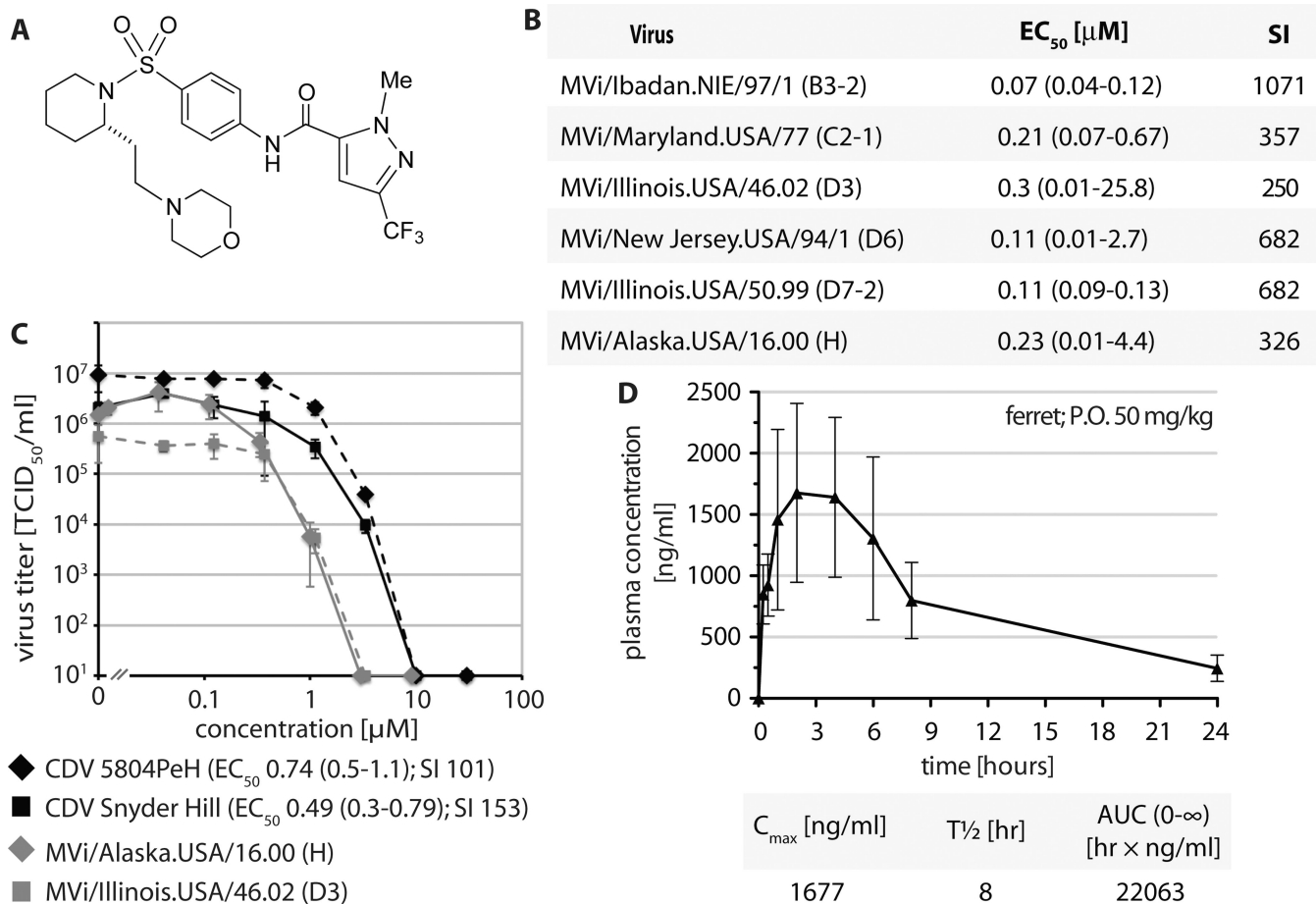


Fig. 1. Identification of a clinical candidate morbillivirus inhibitor for efficacy testing in the CDV/ferret system. **A**) Structure of the lead compound ERDRP-0519. **B**) *In vitro* efficacy testing of ERDRP-0519 against a panel of MeV isolates representing seven distinct, currently endemic genotypes (specified in parentheses). EC₅₀ concentrations were calculated through four-parameter variable slope regression modeling. Values are based on at least three independent experiments for each virus, 95% asymmetrical confidence intervals are shown in parentheses. Specificity indexes (SI) correspond to CC₅₀/EC₅₀. **C**) Dose-response inhibition curves of two pathogenic CDV isolates (5804PeH and Snyder Hill). Two MeV representatives are shown for comparison. EC₅₀ concentrations and SI values were determined as in (B). **D**) Single-dose oral PK study of ERDRP-0519 in ferrets. The article was dosed p.o. in a PEG-200/0.5% methylcellulose (10/90) formulation at 50 mg/kg body mass at zero hours; blood samples were taken at the specified time points post-dosing and drug plasma concentration determined by LC/MS/MS. Shown are mean concentrations (n = 3) ± SEM. Key PK parameters were calculated using the WinNonlin PK software package (C_{max}: maximum observed concentration; t_{1/2}: terminal elimination half-life; AUC_{0-∞}: area under the curve extrapolated to infinity).

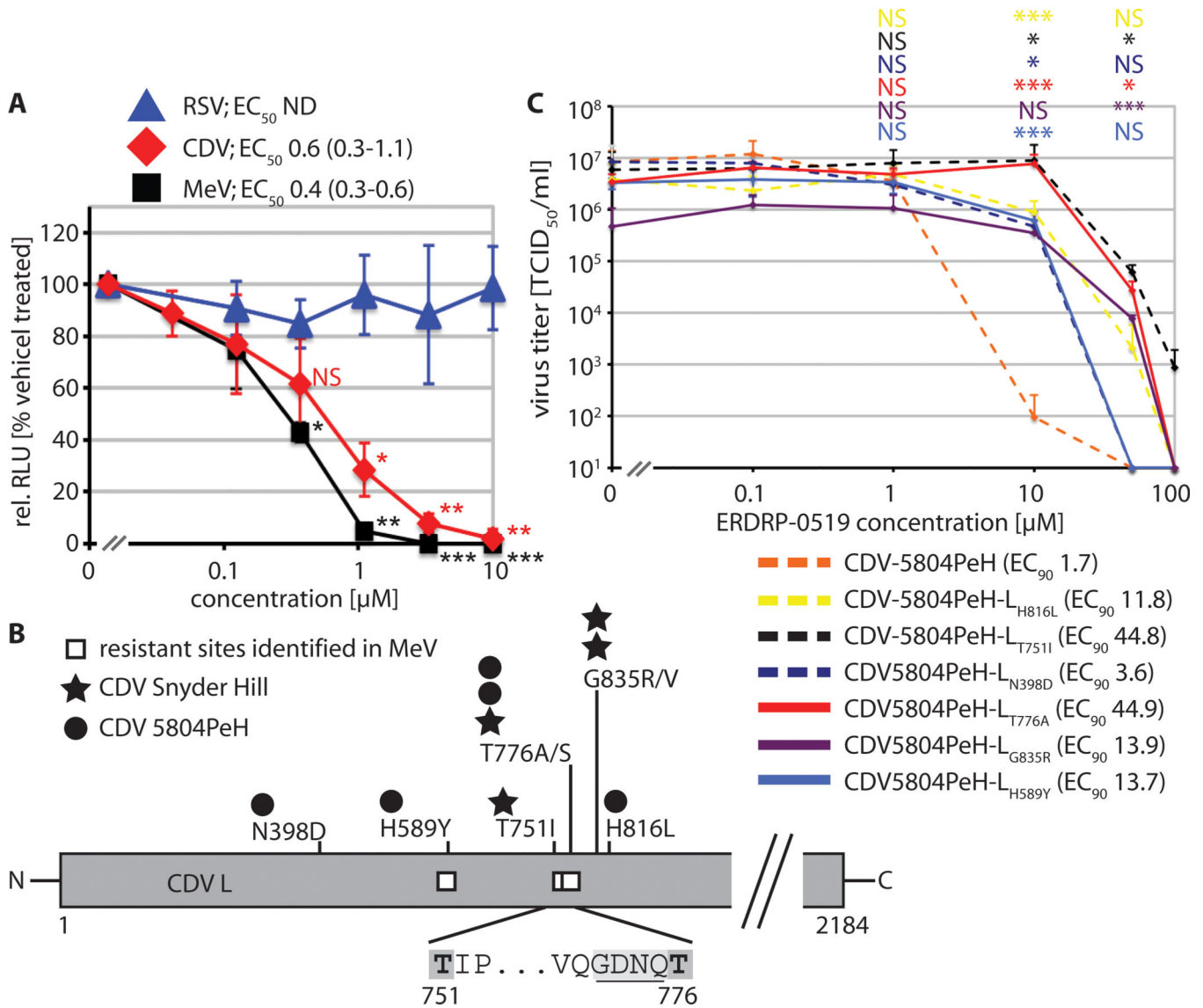


Fig. 2. Mechanism of activity and molecular target of ERDRP-0519 against CDV. **A)** Plasmid-based minigenome luciferase reporter assay to determine bioactivity of RSV, CDV, and MeV polymerase complexes. Relative luciferase units (RLUs) were normalized for values obtained in the presence of vehicle control and represent means of three independent experiments \pm SD. EC₅₀ concentrations and 95% asymmetric confidence intervals were determined as in (fig. 1B). To determine the statistical significance of differences between sample means and values obtained at 0.12 μ M, unpaired two-tailed *t* tests were applied (*: $p < 0.05$; **: $p < 0.01$; ***: $p < 0.001$; NS: not significant). **B)** Summary of confirmed resistance sites identified in the CDV L polymerase subunit through nine independent adaptations of virus strains 5804PeH or Snyder Hill to growth in the presence of ERDRP-0519. Numbers correspond to CDV L amino acid positions. The insert shows the proposed GDNQ catalytic center for phosphodiesterbond formation (underlined), flanked by two resistance sites (dark grey shading). White squares specify mutations previously

identified in MeV L that mediate resistance to an earlier analog of ERDRP-0519 (24). **C** Dose-response inhibition curves of six genetically-controlled CDV-5804PeH recombinants each harboring a single resistance mutant candidate. Values represent mean viral titers of at least three independent experiments \pm SD. Numbers in parentheses specify EC₉₀ concentrations. To test the statistical significance of differences between means of mutant recombinants and standard CDV-5804PeH, unpaired two-tailed *t* tests were applied; symbols as in (A).

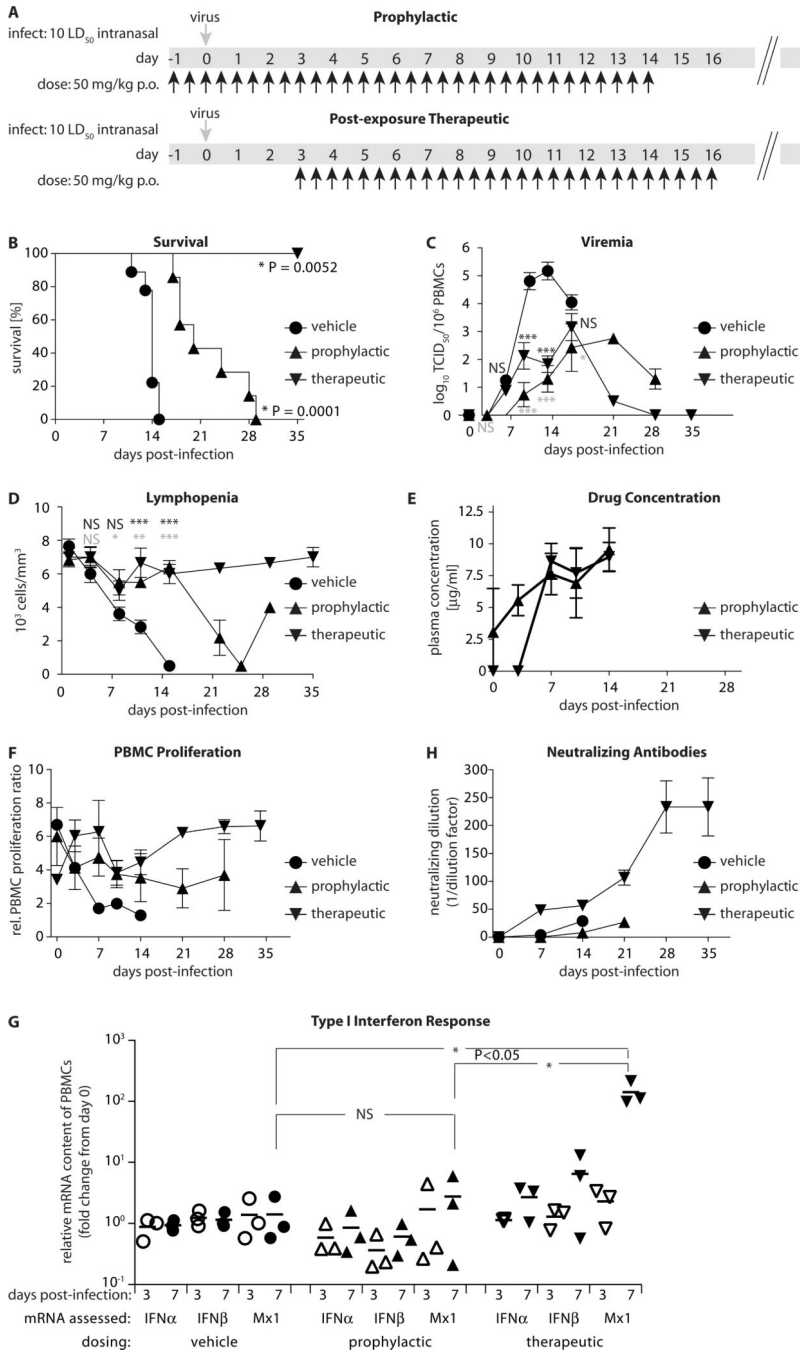


Fig. 3. Oral efficacy assessment of ERDRP-0519 against pathogenic CDV in ferrets. **A)** Prophylactic and PET dosing scheme of ferrets. Animals received ERDRP-0519 orally b.i.d. (black arrows) at 50 mg/kg body mass in a PEG-200/0.5% methylcellulose (10/90) formulation. Controls were dosed with vehicle only. All control animals were dosed with vehicle only following the prophylactic protocol (n=9 (vehicle); n=3 (PET); n=9 (prophylactic)). Virus (1×10⁵ TCID₅₀ units/animal) was given intranasally at day 0 (grey arrows). **B)** Survival curves of animals after prophylactic or PET dosing. Mantel-Cox tests

were applied to assess the statistical significance of differences between the vehicle and treated survival curves. **C)** Cell-associated viremia titers after prophylactic or PET dosing. Values represent means of TCID₅₀ units in 10⁶ isolated PBMCs ± SEM. Bonferroni multiple comparison tests were applied after ANOVA; *: p<0.05; **: p<0.01; ***: p<0.001; NS: not significant; black symbols: PET dosing; grey symbols: prophylactic dosing). **D)** Lymphopenia assessment after prophylactic or PET dosing. Values represent means of lymphocyte counts per mm³ blood ± SEM. Statistical analysis and symbols as in (C). **E)** Multiple-dose drug plasma levels in animals dosed prophylactically or PET. Values represent mean ERDRP-0519 plasma concentrations determined as in (fig. 1D) ± SD. Last sampling at day 14. **F)** Unspecific PBMC proliferation capacity after prophylactic, PET, or vehicle treatment of animals. PBMCs were stimulated with PHA. Values represent mean ratios of BrdU incorporation relative to non-stimulated PBMCs ± SEM. **G)** Induction levels of type I interferon and Mx1 mRNAs in prophylactically, therapeutically, or vehicle-dosed animals at days 0, 3 and 7 post-infection, respectively. PBMCs from three animals per treatment group were analyzed, and values represent relative mRNA fold change in individual animals and means (lines), all normalized for day 0 levels. One-way ANOVA and Tukey's multiple comparison test was applied for statistical analysis. **H)** Neutralizing antibody titers in animals treated prophylactically, PET, or receiving vehicle only. Data represent mean reciprocal dilutions that fully suppressed microscopically detectable CDV cytopathicity ± SEM.

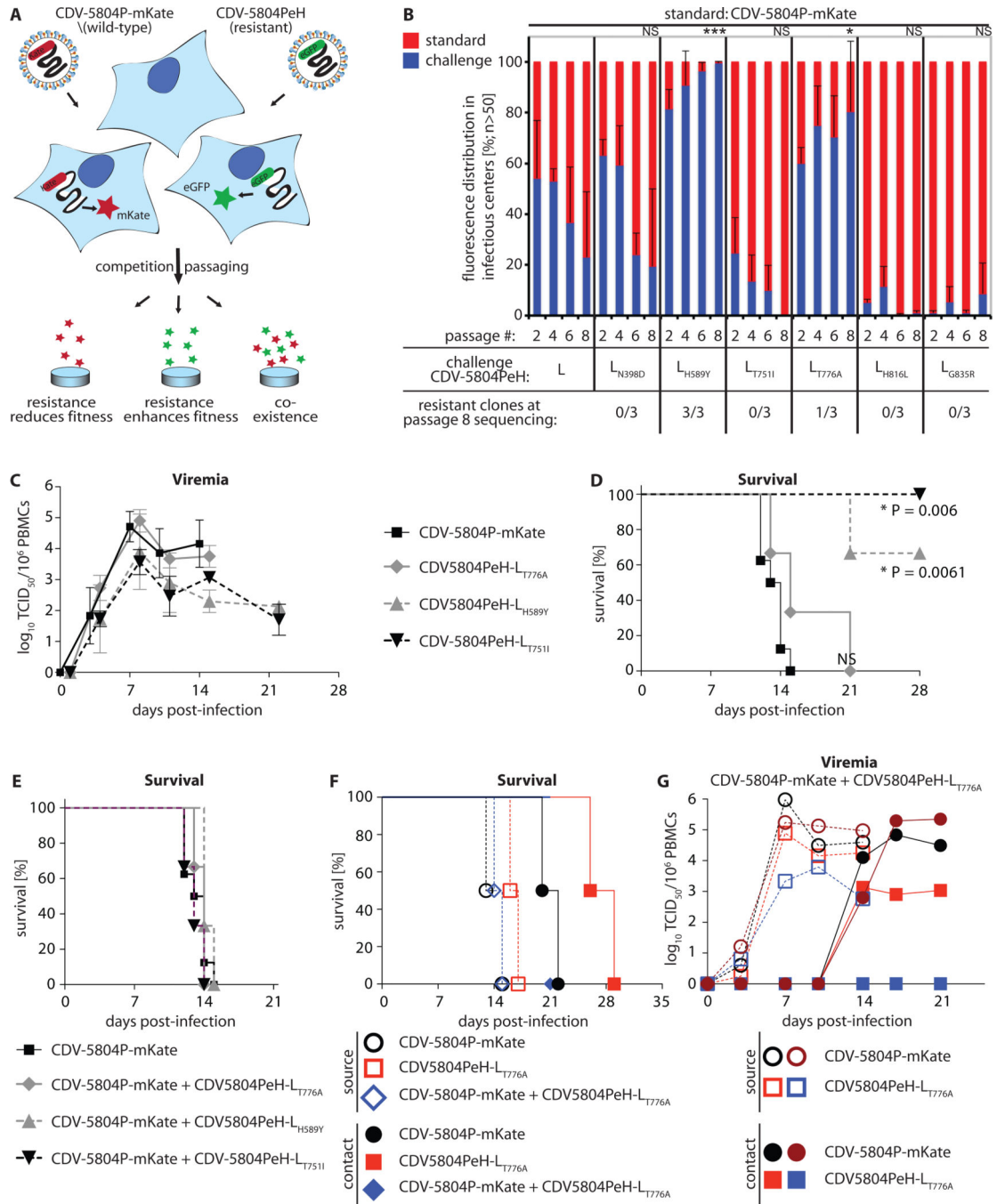


Fig. 4. Resistance package of ERDRP-0519 in the CDV/ferret system. **A)** Schematic of an *in vitro* CDV fitness assay based on co-infection of cells with CDV-5804PeH harboring eGFP or mKate as additional transcription units. Alternative outcomes after repeat passaging are specified. **B)** Relative *in vitro* fitness of six distinct resistant CDV-5804PeH (challenge) compared to parental CDV-5804P-mKate (standard). The relative prevalence of standard and challenge virus was determined based on fluorescence. Values represent mean distributions of three independent experiments each \pm SD. After eight passages, total RNA

was isolated and the prevalent residue at the resistance sites determined. Symbols depict statistical significance of deviation of passage 8 sample means from competition of unmodified CDVs, determined through *t* tests (*: $p < 0.05$; ***: $p < 0.001$; NS: not significant). **C)** Cell-associated viremia titers after intranasal infection with 2×10^5 TCID₅₀ units/animal with standard CDV-5804PeH or resistant variants CDV-5804PeH-L_{T776A}, CDV-5804PeH-L_{H589Y}, or CDV-5804PeH-L_{T751I} ($n = 9$ (CDV-5804PeH); $n = 3$ each for resistant CDVs). Values represent means of TCID₅₀ units in 10^6 isolated PBMCs \pm SD. **D)** Survival curves of animals shown in (C). Mantel-Cox tests were applied to assess the statistical significance of differences between survival of animals infected with standard CDV-5804P-mKate and resistant CDVs. **E)** Survival curves after intranasal infection with 2×10^5 TCID₅₀ units/animal of standard CDV-5804PeH ($n = 9$), or co-infection with 1×10^5 TCID₅₀ units/animal each of CDV-5804P-mKate and a resistant CDV-5804PeH variant ($n = 3$ each). **F)** Contact transmission study. Survival curves of source animals (open symbols) infected with standard CDV-5804P-mKate, resistant CDV-5804PeH-L_{T776A}, or co-infected with both viruses, and the corresponding contact animals (filled symbols). Ferrets were housed in pairs of one source and contact animal (symbols are color matched by co-housed pair; two pairs were tested per virus inoculum). Median survival of contact animals in the CDV-5804P-mKate group was 21 days, in the CDV-5804PeH-L_{T776A} group 27.5 days. **G)** Cell-associated viremia titers in source (open symbols) and contact (filled symbols) animals after intranasal co-infection of source animals with 1×10^5 TCID₅₀ units/animal each of CDV-5804P-mKate and CDV-5804PeH-L_{T776A}. Titers of each virus were determined individually based on fluorescence. Symbols are color matched by co-housed animal pairs and represent viremia titers of individual animals.